ORIGINAL RESEARCH ARTICLE

Journal of Cellular Physiology WILEY

Analysis of lncRNA–mRNA networks after MEK1/2 inhibition based on WGCNA in pancreatic ductal adenocarcinoma

Jing Qian[1]* | Jianxin Yang[2]* | Xianchen Liu[1]* | Zhiming Chen[1] | Xiaodi Yan[1] | Hongmei Gu[1] | Qiang Xue[1] | Xingqin Zhou[1] | Ling Gai[3] | Pengpeng Lu[4] | Yu Shi[1] | Ninghua Yao[1]

[1]Department of Radiotherapy, Affiliated Hospital of Nantong University, Nantong, Jiangsu, China

[2]Department of General Surgery, Qidong People's Hospital, Qidong, Jiangsu, China

[3]Department of Chemotherapy, Affiliated Hospital of Nantong University, Nantong, Jiangsu, China

[4]Department of Oncology, Nantong University, Nantong, Jiangsu, China

Correspondence
Ninghua Yao, Department of Radiotherapy, Affiliated Hospital of Nantong University, Nantong, 226001 Jiangsu, China.
Email: yaonh2009@163.com

Abstract

Pancreatic ductal adenocarcinoma (PDA) responds poorly to treatment. Efforts have been exerted to prolong the survival time of PDA, but the 5-year survival rates remain disappointing. Understanding the molecular mechanisms of PDA development is significant. MEK/ERK pathway signaling has been proven to be important in PDA. lncRNA–mRNA networks have become a vital part of molecular mechanisms in the MEK/ERK pathway. Herein, weighted gene coexpression network analysis was used to investigate the coexpressed lncRNA–mRNA networks in the MEK/ERK pathway based on GSE45765. Differently expressed long noncoding RNA (lncRNA) and messenger RNA (mRNA) were found and 10 modules were identified based on coexpression profiles. Gene ontology and Kyoto Encyclopedia of Genes and Genomes were then performed to analyze the coexpressed lncRNA and mRNA in different modules. PDA cells and tissues were used to validate the analysis results. Finally, we found that NONHSAT185150.1 and B4GALT6 were negatively correlated with MEK1/2. By analyzing GSE45765, the genome-wide profiles of lncRNA–mRNA network after MEK1/2 was established, which might aid the development of drug-targeting MEK1/2 and the investigation of diagnostic markers.

KEYWORDS
lncRNA, MEK1/2, pancreatic ductal adenocarcinoma, WGCNA

1 | INTRODUCTION

Pancreatic ductal adenocarcinoma (PDA) accounts for 95% of pancreatic cancers (Kuroczycki-Saniutycz et al., 2017). About 230,000 new PDA cases are diagnosed worldwide annually (Kuroczycki-Saniutycz et al., 2017; Malats, Molina-Montes, & La Vecchia, 2017). Unfortunately, compared with other malignancies, patients with PDA have the worst 5-year survival rates (Ariake et al., 2017; Kuroczycki-Saniutycz et al., 2017). Delayed diagnosis and lack of effective chemotherapy have been reported as the reasons for such poor rates (Macchini et al., 2019; Sun et al., 2018; Tiriac, Plenker, Baker, & Tuveson, 2019). Thus, understanding the potential molecular mechanism underlying PDA initiation and progression has become increasingly important to enable drug development and diagnostic-marker investigations.

Abbreviations: GO, Gene ontology; KEGG, kyoto Encyclopedia of Genes and Genomes; lncRNA, long noncoding RNAs; PDA, pancreatic ductal adenocarcinoma; qPCR, quantitative reverse transcription polymerase chain reaction; WGCNA, weighted gene coexpression network analysis.

*Jing Qian, Jianxin Yang, and Xianchen Liu contributed equally to this work.

- -

One of the earliest and most common genetic alterations is the activation of the MEK/ERK pathway signaling (Gysin, Paquette, & McMahon, 2012; Kinsey et al., 2019). Previous studies have indicated that the MEK/ERK pathway signaling plays a vital role in the progression of PDA and can become a therapeutic target (Vaseva et al., 2018). Activation of MEK1/ERK1/2 signaling enhances proliferation through apoptosis inhibition (Wang, Zhao et al., 2018). The inhibition of MEK signaling reportedly reduces pancreatic cancer metastasis in mouse models (Gu et al., 2018). A new ERK-specific inhibitor, ulixertinib, has demonstrated an antitumor effect on PDA (Jiang et al., 2018). Accordingly, further understanding the role of the MEK/ERK regulatory network in PDA has become a research hotspot.

Long noncoding RNAs (lncRNAs) are a vital group of noncoding RNA molecules greater than 200 nucleotides (Dong et al., 2019; Yu et al., 2019). Previously, lncRNAs have been regarded as noises of genetic materials (Xiu et al., 2019). However, many studies have proven that lncRNAs play important roles in PDA development (Huang et al., 2018). lncRNA CUDR enhances malignant phenotypes by activating ERK signaling in PDA (Liang et al., 2018). lncRNA NONHSAT105177 induced by melittin suppresses proliferation and migration in PDA (Wang, Li et al., 2018).

The identification of novel lncRNA–mRNA networks can contribute to understanding the potential molecular mechanism underlying oncogenesis and tumor development. Through microarray analyses, a lncRNA–mRNA coexpression network has been constructed in pituitary adenoma. Then, 130 specific lncRNA–mRNA coexpression relationships have been identified, contributing to the investigation of pituitary-adenoma pathogenesis (Xing et al., 2019).

However, genome-wide profiles of lncRNA–mRNA networks in MEK/ERK pathway signaling in PDA are lacking. GSE45765 is expression profiling by using arrays from PDA cells with and without MEK1/2 inhibitor. Thus, in the present work, we downloaded GSE45765 from the GEO database. We then constructed mRNA and lncRNA coexpression networks based on weighted gene coexpression network analysis (WGCNA) and identified 10 modules. Subsequently, function and pathway enrichment analysis were performed through Gene ontology (GO) and Kyoto Encyclopedia of Genes and Genomes (KEGG). Kaplan–Meier survival analysis of differently expressed mRNAs and lncRNAs were performed based on The Cancer Genome Atlas (TCGA). Finally, PDA cell lines and tissues were used to validate the analysis results.

2 | MATERIALS AND METHODS

2.1 | Data processing

The gene-expression profile GSE45765 provided by Gysin et al (https://www.gcbi.com.cn/gcbi/dataplus/html/details?acc=GSE45765&keywords=GSE45765) was obtained from the Gene Expression Omnibus (GEO) database. Eight PDA cell samples were thereafter downloaded with or without MEK1/2 inhibition. The raw files were processed with robust multiarray average (RMA) algorithm. The
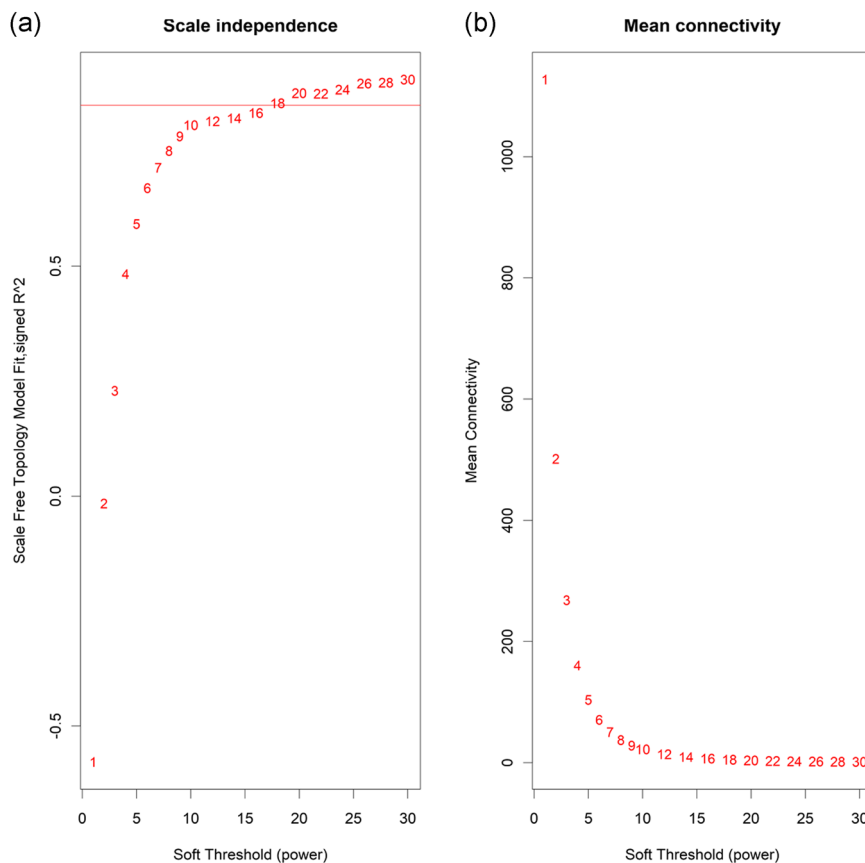

FIGURE 1 Freedom relative weight choice about coexpression modules. Numbers in the plots show the corresponding soft thresholding powers. The approximate freedom relative weight choice can be attained at the soft thresholding power of 18
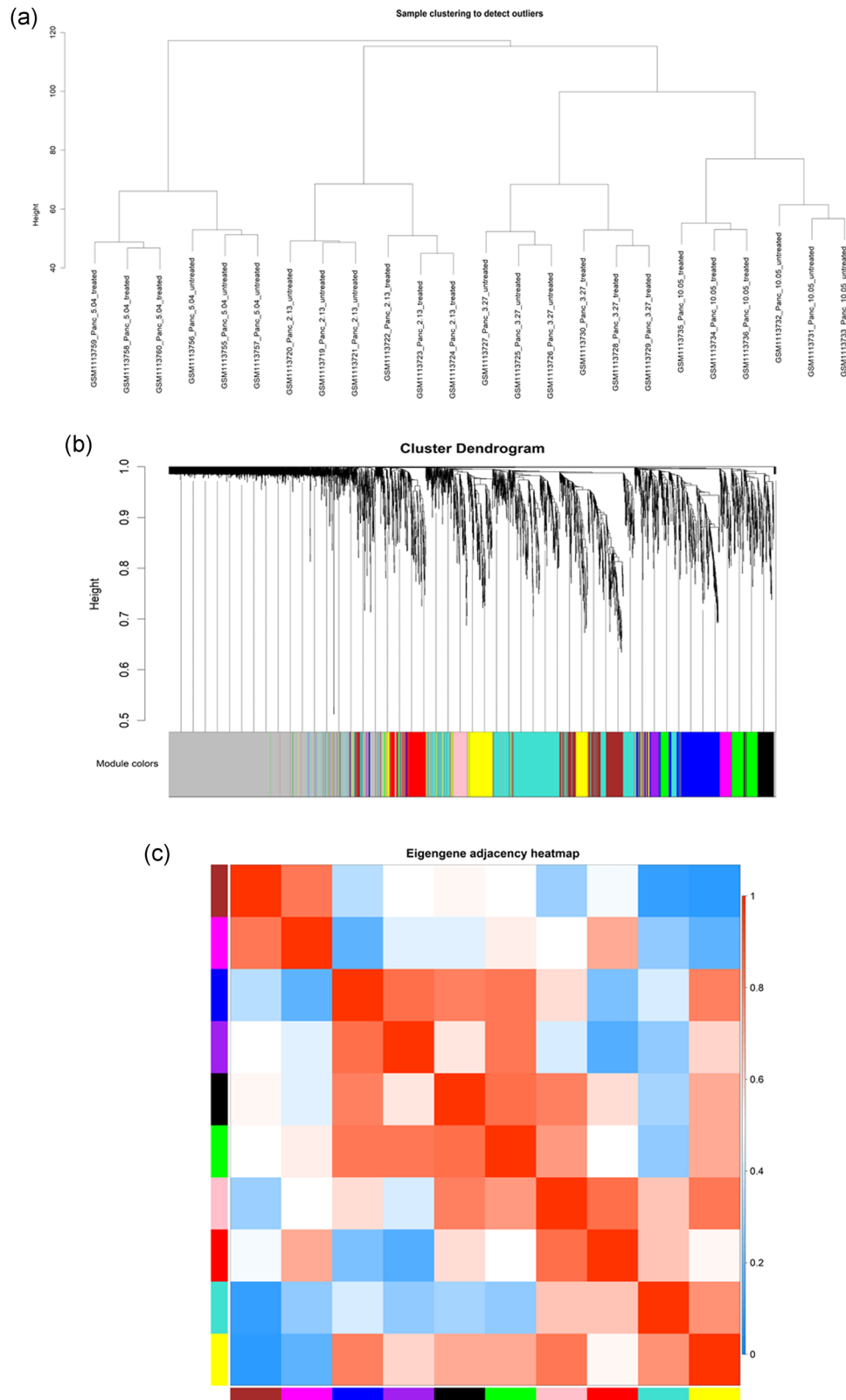
FIGURE 2 lncRNA and mRNA coexpression modules identified by WGCNA. (a) Dendrogram of bioinformatics analysis based on GSE45765. (b) Dendrogram obtained by clustering the dissimilarity based on consensus topological overlap with the corresponding module colors indicated by the color row. (c) Eigengene adjacencies of heat map. Red shows high adjacency and blue shows low adjacency. lncRNA, long noncoding RNA; mRNA, messenger RNA; WGCNA, weighted gene coexpression network analysis

Module-trait relationships

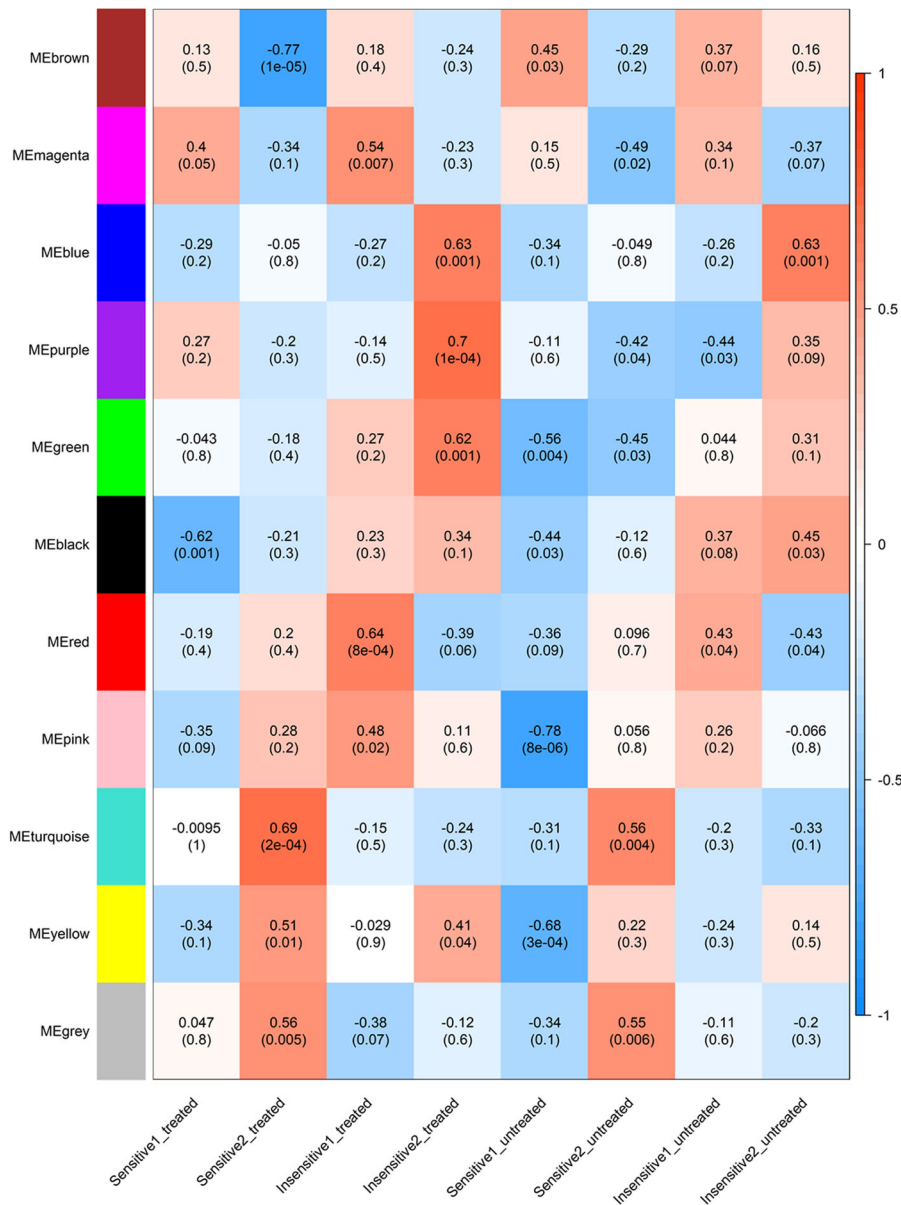|	Sensitive1_treated	Sensitive2_treated	Insensitive1_treated	Insensitive2_treated	Sensitive1_untreated	Sensitive2_untreated	Insensitive1_untreated	Insensitive2_untreated
MEbrown	0.13 (0.5)	-0.77 (1e-05)	0.18 (0.4)	-0.24 (0.3)	0.45 (0.03)	-0.29 (0.2)	0.37 (0.07)	0.16 (0.5)
MEmagenta	0.4 (0.05)	-0.34 (0.1)	0.54 (0.007)	-0.23 (0.3)	0.15 (0.5)	-0.49 (0.02)	0.34 (0.1)	-0.37 (0.07)
MEblue	-0.29 (0.2)	-0.05 (0.8)	-0.27 (0.2)	0.63 (0.001)	-0.34 (0.1)	-0.049 (0.8)	-0.26 (0.2)	0.63 (0.001)
MEpurple	0.27 (0.2)	-0.2 (0.3)	-0.14 (0.5)	0.7 (1e-04)	-0.11 (0.6)	-0.42 (0.04)	-0.44 (0.03)	0.35 (0.09)
MEgreen	-0.043 (0.8)	-0.18 (0.4)	0.27 (0.2)	0.62 (0.001)	-0.56 (0.004)	-0.45 (0.03)	0.044 (0.8)	0.31 (0.1)
MEblack	-0.62 (0.001)	-0.21 (0.3)	0.23 (0.3)	0.34 (0.1)	-0.44 (0.03)	-0.12 (0.6)	0.37 (0.08)	0.45 (0.03)
MEred	-0.19 (0.4)	0.2 (0.4)	0.64 (8e-04)	-0.39 (0.06)	-0.36 (0.09)	0.096 (0.7)	0.43 (0.04)	-0.43 (0.04)
MEpink	-0.35 (0.09)	0.28 (0.2)	0.48 (0.02)	0.11 (0.6)	-0.78 (8e-06)	0.056 (0.8)	0.26 (0.2)	-0.066 (0.8)
MEturquoise	-0.0095 (1)	0.69 (2e-04)	-0.15 (0.5)	-0.24 (0.3)	-0.31 (0.1)	0.56 (0.004)	-0.2 (0.3)	-0.33 (0.1)
MEyellow	-0.34 (0.1)	0.51 (0.01)	-0.029 (0.9)	0.41 (0.04)	-0.68 (3e-04)	0.22 (0.3)	-0.24 (0.3)	0.14 (0.5)
MEgrey	0.047 (0.8)	0.56 (0.005)	-0.38 (0.07)	-0.12 (0.6)	-0.34 (0.1)	0.55 (0.006)	-0.11 (0.6)	-0.2 (0.3)

FIGURE 3 Relationships of consensus module-trait in lncRNA and mRNA coexpression modules. According to the corresponding color legend, the table was color-coded to show the correlation. Specifically, red showed a positive correlation and blue showed a negative correlation. The corresponding numbers in squares showed the correlation between the module stage and eigengenes. The corresponding *p* values are shown below in parentheses. lncRNA, long noncoding RNA; mRNA, messenger RNA

nsFilter algorithm was used to filter the data for the subsequent WGCNA. All data used for Kaplan–Meier survival analysis were obtained from TCGA (https://www.cancer.gov/about-nci/organization/ccg/research/structural-genomics/tcga). The clinical features of patients from TCGA are provided in the Supporting Information, and Kaplan–Meier survival analysis was performed based on TCGA.

2.2 | Patients and tissue specimens

Patients with PDA were enrolled at the Affiliated Hospital of Nantong University and Qidong People's Hospital from 2016 to 2018. PDA tissue samples were frozen in liquid nitrogen. Approaches used in the study were approved by the Ethics Committee (No. 2013 [22]) of Nantong University and conformed with the *Ethical Guidelines of the 1975 Declaration of Helsinki* (6th revision, 2008) and government policies.

2.3 | Cell lines and culture conditions

PaCa-2 and Panc-1 were cultured in an incubator (37°C, 5% CO_2) and in RPMI 1640 (Gibco) supplemented with 10% fetal bovine serum (Gibco). PDA cells were treated by CI-1040 following literature [Huang et al., 2018].

2.4 | Cell transfection

siRNA-MEK1 and siRNA-MEK2 were transfected into PaCa-2 and Panc-1. The empty vector functioned as a negative control. Lipofectamine 2000 (Invitrogen) was used for the transfection according to the official instructions.
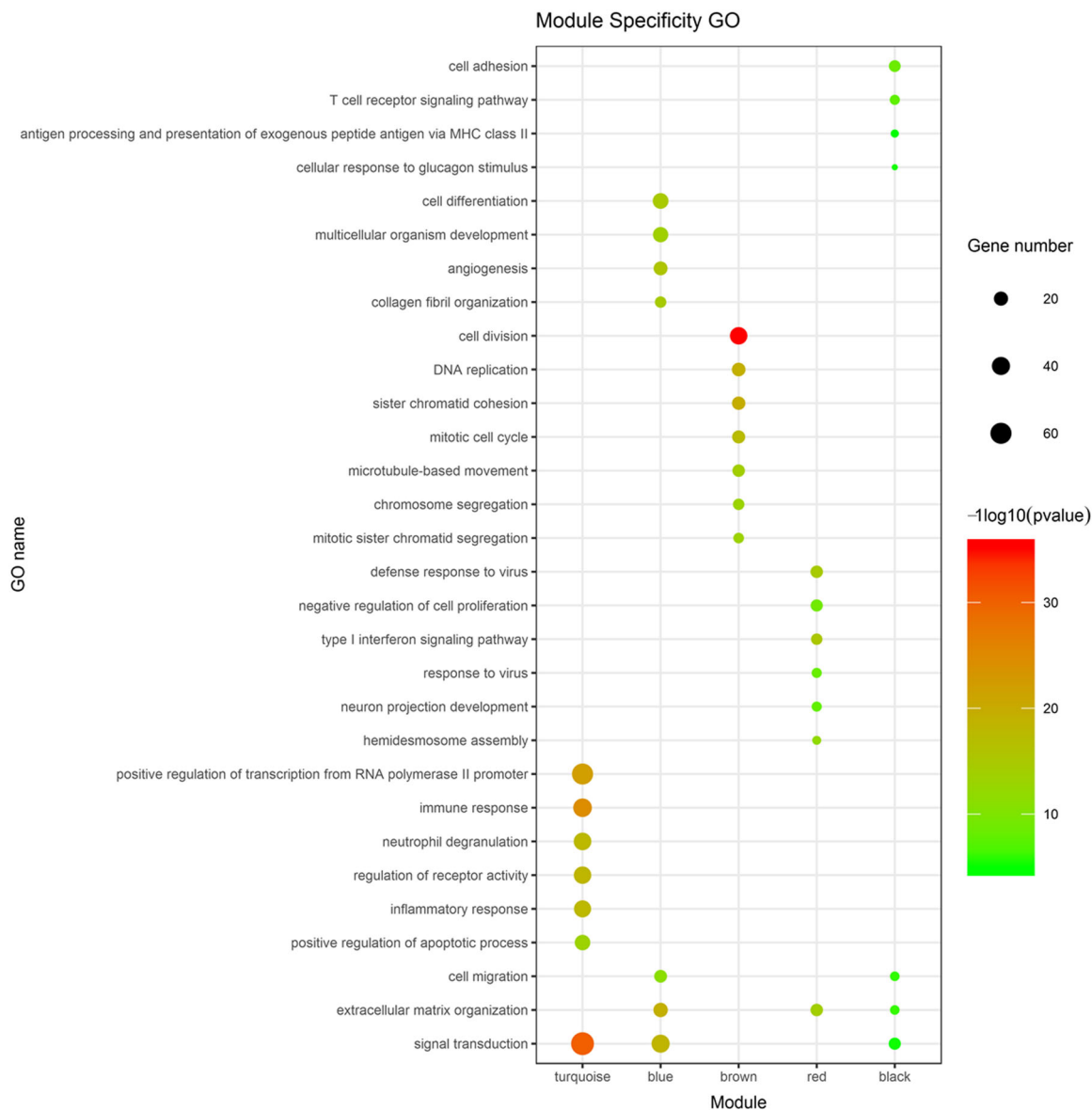
FIGURE 4 Result of GO analysis about mRNA based on WGCNA. The vertical axis shows the results of the GO analysis and the horizontal axis shows the different modules. The color of the round shape shows transitional values (log10 of q value), and the size shows the number of genes that were enriched. Go, Gene ontology; mRNA, messenger RNA; WGCNA, weighted gene coexpression network analysis

2.5 | Quantitative reverse-transcription polymerase chain reaction

All RNAs were isolated using TRIzol Reagent (Life Technologies). SYBR Green qRT-PCR on an ABI7300 real-time PCR machine was used to measure the expression levels of mRNAs. B4GALT6B4GALT6 and β-actin expression were examined using the following specific primers: 5′ CGGATGATGCGGGTTTCCAA3′, 5′ACCGTTGAGCGTACTGTTTTTA3′, 5′GGACTTCGAGCAAGAGATGG3′, and 5′AGCACTGTGTTGGCGT ACAG3′.

2.6 | Establishment of weighted gene coexpression networks and identification of modules

lncRNA–mRNA coexpression networks and modules were constructed according to literature (Yin, Cai, Zhu, & Xu, 2018). WGCNA is a freely accessible R package for the construction of weighted lncRNA–mRNA coexpression networks. In the present research, a one-step function was performed to construct network and detect consensus modules.
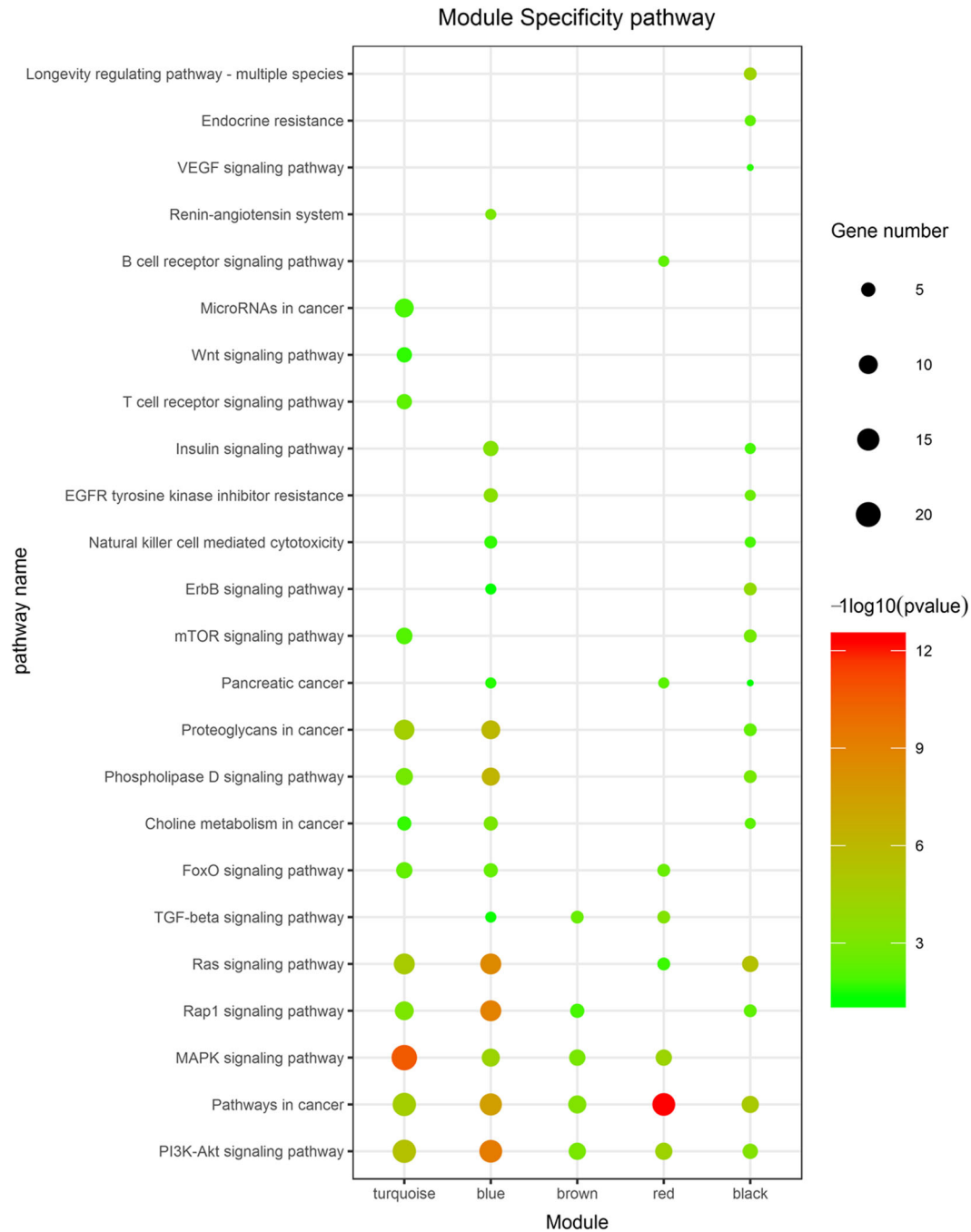
Module Specificity pathway

FIGURE 5 Result of pathway analysis about mRNA based on WGCNA. The vertical axis shows the results of pathway analysis and the horizontal axis shows the different modules. The color of the round shape shows transitional values (log10 of q value), and the size shows the number of genes that were enriched. mRNA, messenger RNA; WGCNA, weighted gene coexpression network analysis

2.7 | Interaction analysis of coexpression modules

The interaction analysis of coexpression modules was performed following literature (Wang, Xu et al., 2018). We calculated the eigengene adjacency, which was based on similar coexpression in modules. The specific interaction relationship among different modules was processed through flashClust function. A heat map was established to show the correlations of different modules.

2.8 | GO function and KEGG pathway analyses

GO function and KEGG pathway analyses were performed following literature (Wang, Xu et al., 2018). GO function and KEGG pathway analyses were performed using discovery (DAVID) and KOBAS 3.0. R language ggplot2 package was used to process the enrichment results of visualization figures.

TABLE 1 The result of lncRNA–mRNA pathway about differently expressed lncRNAs

Module	lncRNA	Style	p
Turquoise	NONHSAT185150.1	Up	.012
Turquoise	NR_136202.1	Up	.018
Turquoise	NONHSAT033101.2	Up	.043
Red	ENST00000381105.2	Down	.023
Red	ENST00000614781.1	Up	.0081
Red	NONHSAT108374.2	Up	.0029
Black	NONHSAT040789.2	Down	.031
Black	ENST00000633336.1	Up	.020
Black	NONHSAT097188.2	Up	.026

Abbreviations: lncRNA, long noncoding RNA; mRNA, messenger RNA.

3 | RESULTS

3.1 | Data of GSE4576 processing

Eight PDA cell sample raw files were obtained from NCBI (https://www.ncbi.nlm.nih.gov/pubmed/). The expression profiles by an array of GSE4576 were converted to expression data, which was handled with the RMA algorithm. Specifically, the RMA algorithm included background correction, normalization, and summarization based on R language programming. The differently expressed mRNAs and lncRNAs are listed in the Supporting Information.

3.2 | Establishing weighted lncRNA–mRNA coexpression networks and identification of soft threshold power

A lncRNA–mRNA coexpression network was established from the sample raw files, and different modules were established. Soft threshold power 18 was used to define the adjacency matrix, which was processed with the criteria of approximate scale-free topology (Figure 1).

TABLE 2 The part result of lncRNA–mRNA pathway about differently expressed mRNA

Module	mRNA	Style	p
Turquoise	CXCL3	Up	.00052
Turquoise	CDC6	Down	.0014
Turquoise	FAXDC2	Up	.0069
Black	B4GALT6	Down	.038
Black	MPDZ	Up	.021
Black	AMY1A	Up	.00052
Red	DAPK1	Up	.0089
Red	INPP5B	Down	.042
Red	LAMA3	Up	.0046

Abbreviations: lncRNA, long noncoding RNA; mRNA, messenger RNA.

3.3 | Correlation among different modules

A dendrogram of bioinformatics analysis based on GSE45765 is shown in Figure 2a. Dendrogram clusters and heat maps are shown in Figure 2b,c. The minimum module size was 10, the module detection sensitivity deepSplit was 2, and the cut height for merging of modules was 0.2, indicating that the modules whose eigengenes were correlated above 0.8 will be merged. Combined with Figure 3, various modules related to MEK/ERK signaling were found. For example, green, black, red, turquoise, pink, yellow, and blue modules were related to MEK1/2 inhibition. Specifically, the red module meant intense relation to insensitive cells and black meant strong relation to sensitive cells.

3.4 | GO function and KEGG pathway analyses

Based on differently expressed mRNAs, GO function and KEGG pathway analysis were performed (Figures 4 and 5). GO function analysis indicated that differently expressed mRNAs were enriched during tumor progression. For example, blue module meant enrichment in function on cell migration, red module meant enrichment in function on proliferation, and turquoise module meant enrichment in function on cell apoptosis (Figure 4). Similarly, KEGG pathway analysis showed that MEK/ERK-related pathways and other vital cancer pathways were enriched. For example, Ras and MAPK pathways were enriched isun turquoise, blue, and red modules. PI3K-AKT pathway was enriched in turquoise, blue, brown, red, and black modules (Figure 5).

3.5 | Construction of lncRNA–mRNA network and lncRNA–mRNA pathway

Using GSE45765 data, lncRNA and mRNA coexpress networks were established based on the WGCNA method. The selection results of differently expressed lncRNAs and mRNA are shown in Tables 1 and 2. The lncRNA–mRNA network in black (a), red (b), and turquoise (c) modules are shown in Figure 6a–c, and the lncRNA–mRNA pathway in black (d), red (e), and turquoise (f) are shown in Figure 6d–f. lncRNA and mRNA coexpression networks were enriched in the pathway related to MEK/ERK pathway signaling and in multiple-cancer pathway signaling. For example, RAS pathway signaling and MAPK pathway signaling was strongly correlated with MEK/ERK pathway signaling (Diamond et al., 2019; Xie et al., 2019). Rap1 pathway, PI3K/AKT pathway, and JAK/STAT pathway were closely related to cancer progression (Hamidi & Ivaska, 2018). These results suggested that MEK1/2 was a central location in progression of PDA and can thus contribute to investigating the potential relationship between MEK/ERK pathway signaling and other multiple cancer-related pathways.
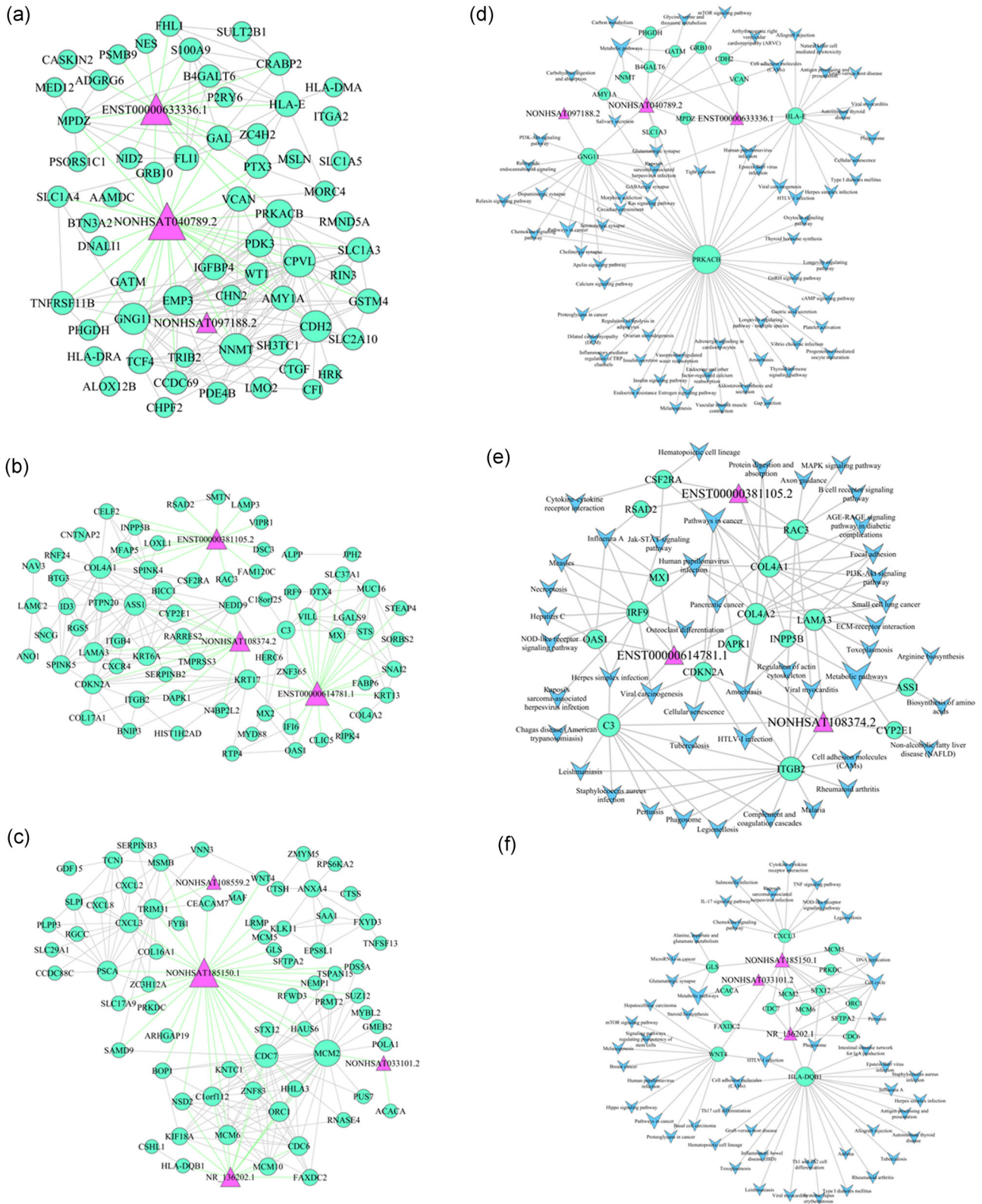
FIGURE 6 Established lncRNA–mRNA network and lncRNA–mRNA pathway. (a–c) lncRNA–mRNA network of genes in black (a), red (b), and turquoise (c) modules. (d–f) lncRNA–mRNA pathway of genes in black (d), red (e), and turquoise (f) modules
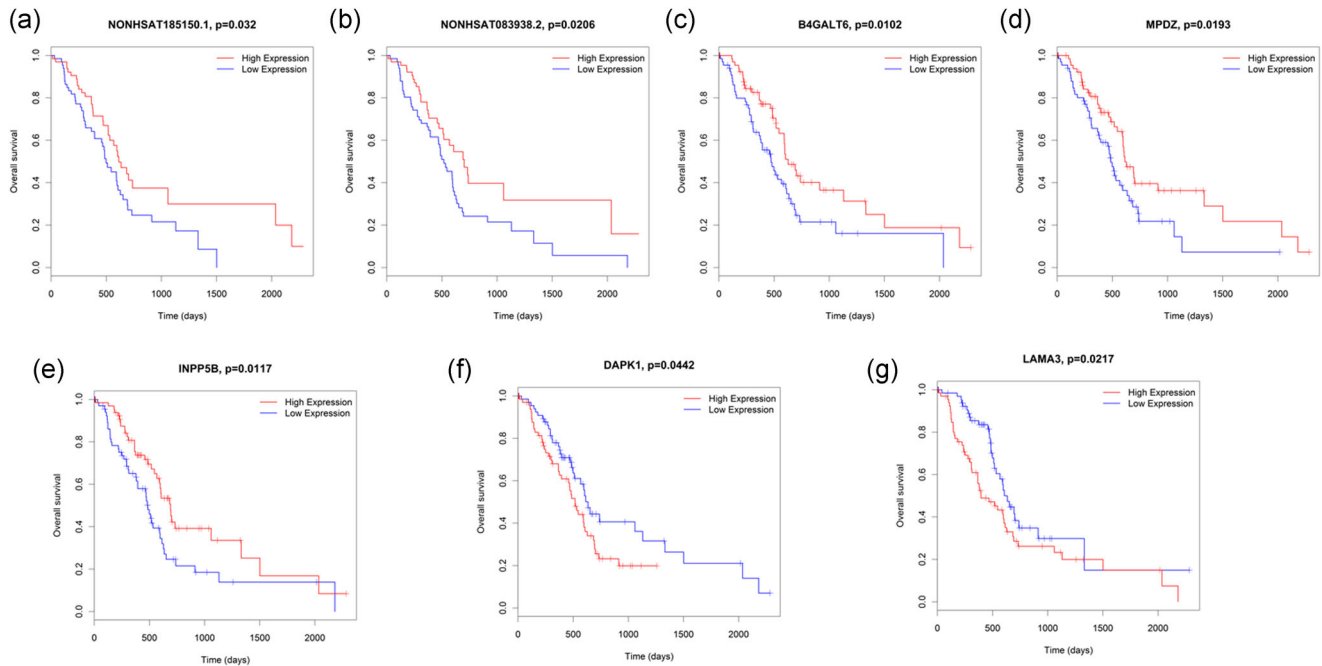
FIGURE 7 Kaplan–Meier survival analysis of lncRNAs and genes. (a, b) High NONHSAT185150.1 and NONHSAT083938.2 expression were significantly associated positively with OS in PDA. (c–e) High B4GALT6, MPDZ, and INPP5B expression were positively associated with OS in PDA. (f, g) High DAPK1 and LAMA3 were negatively associated with OS in PDA. lncRNA, long noncoding RNA; OS, overall survival; PDA, pancreatic ductal adenocarcinoma

3.6 | Kaplan–Meier survival analysis

MEK1/2 was negatively correlated with the overall survival of PDA. Based on TCGA, Kaplan–Meier survival analysis was used to determine the relationship of the expression levels of lncRNAs and genes with the survival time of PDA. The survival data was provided in the Supporting Information. As shown in Figure 7, NONHSAT185150.1 and NON-HSAT083938.2 were positively correlated with the overall survival of PDA (Figure 7a,b). Moreover, B4GALT6, MPDZ, and INPP5B were positively correlated with the overall survival of PDA (Figure 7c–f). DAPK1 and LAMA3 were negatively correlated with the overall survival of PDA (Figure 7f,g). Thus, above lncRNAs and mRNA may play important roles in MEK/ERK pathway signaling and can be prognostic markers for PDA.

3.7 | The expression levels of NONHSAT185150.1 and B4GALT6 were negatively correlated with MEK1/2

To validate the results of coexpression network, qPCR was performed. Results indicated that NONHSAT185150.1 expression levels were upregulated in PaCa-2 and Panc-1 treated by CI-1040 (Figure 8a,b). Similarly, B4GALT6 expression levels were upregulated in PDA treated by CI-1040 (Figure 8c,d). Moreover, western blot results indicated that the protein expression levels of B4GALT6 were upregulated in PDA cells treated by CI-1040 (Figure 8e). According to the expression level of MEK1/2, PDA tissues were divided into two groups. qPCR results indicated that NONHSAT185150.1 expression level was negatively correlated with MEK1/2 in PDA tissues (Figures 8f,g), and the B4GALT6

expression level was negatively correlated to MEK1/2 in PDA tissues (Figure 8h,i).

4 | DISCUSSION

Early-stage diagnostic markers and effective drugs for PDA are unavailable, so the molecular mechanism of PDA progression needs to be understood. The MEK/ERK pathway has been recently considered as a breakthrough point in PDA. The new drug targeting this pathway has been subjected to clinical experiments (Jiang et al., 2018). lncRNAs are important regulators of gene expression and play vital roles in cancer. HOXD-AS1 upregulates the expression of PIK3R3 by competing endogenous RNAs in ovarian cancer (Dong et al., 2019). A positive feedback loop exists between HOTAIR and EZH2 in prostate cancer (Ling et al., 2017). The lncRNA–mRNA network has provided a new angle to understand cancer-related pathways (Jia et al., 2019). In the present study, the lncRNA–mRNA network after MEK1/2 inhibition was established based on WGCNA.

GSE45765, which is the genome-wide profile after MEK1/2 inhibition, was initially obtained from GEO. Differently expressed lncRNAs and mRNAs were found and 10 modules were identified based on WGCNA. The relationship among consensus module traits were then studied. Many modules showed strong relevance after MEK1/2 inhibition. Specifically, the red module was intensely correlated with insensitive cells and black was strongly correlated with sensitive cells. Moreover, GO and pathway analyses were performed based on differently expressed genes. Interestingly, the
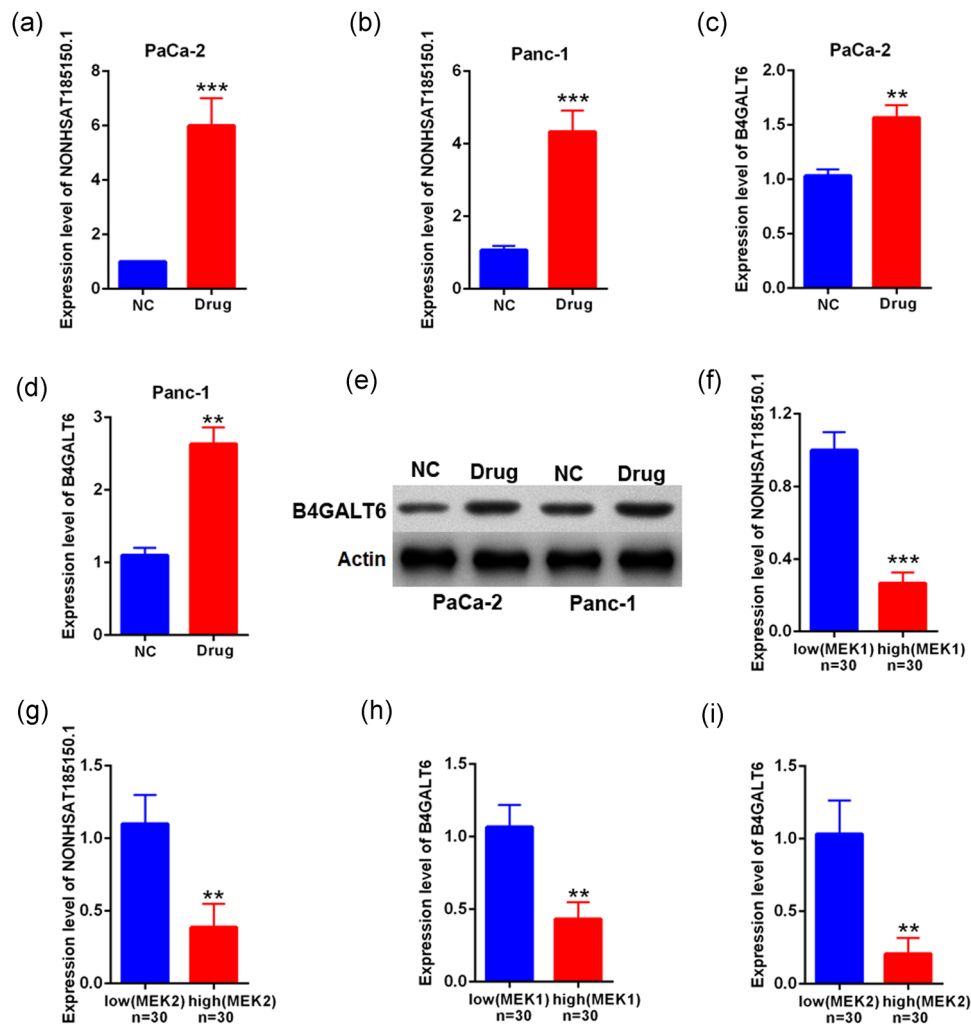
FIGURE 8 The expression level of NONHSAT185150.1 and B4GALT6 was negatively correlated with MEK1/2. (a, b) The expression level of NONHSAT185150.1 was upregulated after MEK1/2 inhibition in PAD cells. (c, d) The expression level of B4GALT6 was upregulated after MEK1/2 inhibition in PAD cells. (e) Western blot results indicated that the protein expression levels of B4GALT6 were upregulated in PDA cells treated by CI-1040. (f, g) The expression level of NONHSAT185150.1 was negatively correlated with MEK1/2 in PAD tissues. (h, i) The expression level of B4GALT6 was negatively correlated with MEK1/2 in PAD tissues

analysis results included the MEK/ERK1-related pathway (RAS and MAPK pathways) and many other cancer-related pathways (FoxO and mTOR pathways). All these results suggested that MEK1/2 may be the trigger in various pathways. Moreover, the lncRNA–mRNA network and lncRNA–mRNA pathway network were established. Nine new lncRNAs were identified in selected modules. lncRNAs can upregulate or downregulate gene expression in several manners (Gao et al., 2019). A total of 44 coexpressed mRNA were identified. For instance, DAPK1, CDH2, WNT4, and RSAD2 are downstream signaling molecules of the MEK/ERK pathway (Civiero, Dihanich, Lewis, & Greggio, 2014; Su, Li, Shi, Hruban, & Radice, 2016). ASS1, CDKN2A, and RAC3 also play important roles in PDA progression (Lowery et al., 2017). Apart from the MEK/ERK-related pathways such as 1 and 2, other cancer-related pathways exist in the network. Thus, the lncRNA–mRNA pathway network can help investigate the roles of MEK1/2 in the regulatory network in PDA. Finally, PDA cells and

tissues were used to validate the coexpression network. After treatment with CI-1040, qRCR results showed that NON-HSAT185150.1 expression levels were upregulated in PaCa-2 and Panc-1. Similarly, B4GALT6 mRNA expression levels were upregulated in PaCa-2 and Panc-1. PDA tissues ($n = 60$) were further divided into two groups following the B4GALT6 expression level. qPCR results indicated that the expression levels of NONHSAT185150.1 and B4GALT6 were negatively related to the MEK1/2 expression level.

In conclusion, this study presented a lncRNA–mRNA network after MEK1/2 inhibition at the genome level based on WGCNA. Ten modules were identified using WGCNA. GO and pathway analyses were performed based on differently expressed genes. Furthermore, lncRNA–mRNA network and lncRNA–mRNA pathway network were established in three selected modules. qPCR results indicated that NONHSAT185150.1 and B4GALT6 were negatively correlated with MEK1/2 expression level in PDA cells and tissues. Overall, our study

can help explore the MEK/ERK pathway and study the drug targeting of MEK1/2.

ACKNOWLEDGMENT

CONFLICT OF INTEREST

The authors declare that there is no conflict of interest.

AUTHOR CONTRIBUTIONS

N. Y. contributed to the conception and design of the study. J. Q., J. Y., and X. L. conceived and designed the study, analyzed the data, drafted, and revised the manuscript. Z. C., X. Y., H. G., and Q. X. participated in the study design, data acquisition, and the quality control of data. X. Z., L. G., P. L., and Y. S. contributed to the study conception, collection and interpretation of data, and critical revision of the manuscript.

ORCID

Ninghua Yao http://orcid.org/0000-0001-9046-0200

REFERENCES

Ariake, K., Motoi, F., Ohtsuka, H., Fukase, K., Masuda, K., Mizuma, M., ... Unno, M. (2017). Predictive risk factors for peritoneal recurrence after pancreatic cancer resection and strategies for its prevention. *Surgery Today, 47*(12), 1434–1442.

Civiero, L., Dihanich, S., Lewis, P. A., & Greggio, E. (2014). Genetic, structural, and molecular insights into the function of ras of complex proteins domains. *Chemistry & Biology, 21*(7), 809–818.

Diamond, E. L., Durham, B. H., Ulaner, G. A., Drill, E., Buthorn, J., Ki, M., ... Hyman, D. M. (2019). Efficacy of MEK inhibition in patients with histiocytic neoplasms. *Nature, 567*(7749), 521–524.

Dong, S., Wang, R., Wang, H., Ding, Q., Zhou, X., Wang, J., ... Zeng, Y. (2019). HOXD-AS1 promotes the epithelial to mesenchymal transition of ovarian cancer cells by regulating miR-186-5p and PIK3R3. *Journal of Experimental & Clinical Cancer Research, 38*(1), 110.

Gao, R., Zhang, N., Yang, J., Zhu, Y., Zhang, Z., Wang, J., ... Bi, J. (2019). Long non-coding RNA ZEB1-AS1 regulates miR-200b/FSCN1 signaling and enhances migration and invasion induced by TGF-β1 in bladder cancer cells. *Journal of Experimental & Clinical Cancer Research, 38*(1), 111.

Gu, D., Lin, H., Zhang, X., Fan, Q., Chen, S., Shahda, S., ... Xie, J. (2018). Simultaneous inhibition of MEK and Hh signaling reduces pancreatic cancer metastasis. *Cancers, 10*(11), E403.

Gysin, S., Paquette, J., & McMahon, M. (2012). Analysis of mRNA profiles after MEK1/2 inhibition in human pancreatic cancer cell lines reveals pathways involved in drug sensitivity. *Molecular Cancer Research, 10*(12), 1607–1619.

Hamidi, H., & Ivaska, J. (2018). Every step of the way: Integrins in cancer progression and metastasis. *Nature Reviews Cancer, 18*(9), 533–548.

Huang, F., Chen, W., Peng, J., Li, Y., Zhuang, Y., Zhu, Z., ... Zhang, S. (2018). LncRNA PVT1 triggers cyto-protective autophagy and promotes pancreatic ductal adenocarcinoma development via the miR-20a-5p/ULK1 Axis. *Molecular Cancer, 17*(1), 98.

Jia, L., Zhang, Y., Ji, Y., Li, X., Xing, Y., Wen, Y., ... Xu, X. (2019). Comparative analysis of lncRNA and mRNA expression profiles between periodontal ligament stem cells and gingival mesenchymal stem cells. *Gene, 699*, 155–164.

Jiang, H., Xu, M., Li, L., Grierson, P., Dodhiawala, P., Highkin, M., ... Lim, K. H. (2018). Concurrent HER or PI3K inhibition potentiates the antitumor effect of the ERK inhibitor ulixertinib in preclinical pancreatic cancer models. *Molecular Cancer Therapeutics, 17*(10), 2144–2155.

Kinsey, C. G., Camolotto, S. A., Boespflug, A. M., Guillen, K. P., Foth, M., Truong, A., ... McMahon, M. (2019). Protective autophagy elicited by RAF→MEK→ERK inhibition suggests a treatment strategy for RAS-driven cancers. *Nature Medicine, 25*(4), 620–627.

Kuroczycki-Saniutycz, S., Grzeszczuk, A., Zwierz, Z. W., Kołodziejczyk, P., Szczesiul, J., Zalewska-Szajda, B., ... Szajda, S. D. (2017). Prevention of pancreatic cancer. *Contemporary Oncology, 21*(1), 30–34.

Liang, X., Qi, M., Wu, R., Liu, A., Chen, D., Tang, L., ... Shao, C. (2018). Long non-coding RNA CUDR promotes malignant phenotypes in pancreatic ductal adenocarcinoma via activating AKT and ERK signaling pathways. *International Journal of Oncology, 53*(6), 2671–2682.

Ling, Z., Wang, X., Tao, T., Zhang, L., Guan, H., You, Z., ... Chen, M. (2017). Involvement of aberrantly activated HOTAIR/EZH2/miR-193a feedback loop in progression of prostate cancer. *Journal of Experimental & Clinical Cancer Research, 36*(1), 159.

Lowery, M. A., Yu, K. H., Kelsen, D. P., Harding, J. J., Bomalaski, J. S., Glassman, D. C., ... O'Reilly, E. M. (2017). A phase 1/1B trial of ADI-PEG 20 plus nab-paclitaxel and gemcitabine in patients with advanced pancreatic adenocarcinoma. *Cancer, 123*(23), 4556–4565.

Macchini, M., Chiaravalli, M., Zanon, S., Peretti, U., Mazza, E., Gianni, L., & Reni, M. (2019). Chemotherapy in elderly patients with pancreatic cancer: Efficacy, feasibility and future perspectives. *Cancer Treatment Reviews, 72*, 1–6.

Malats, N., Molina-Montes, E., & La Vecchia, C. (2017). Genomics in primary and secondary prevention of pancreatic cancer. *Public Health Genomics, 20*(2), 92–99.

Su, Y., Li, J., Shi, C., Hruban, R. H., & Radice, G. L. (2016). N-cadherin functions as a growth suppressor in a model of K-ras-induced PanIN. *Oncogene, 35*(25), 3335–3341.

Sun, Q., Zhang, B., Hu, Q., Qin, Y., Xu, W., Liu, W., ... Xu, J. (2018). The impact of cancer-associated fibroblasts on major hallmarks of pancreatic cancer. *Theranostics, 8*(18), 5072–5087.

Tiriac, H., Plenker, D., Baker, L. A., & Tuveson, D. A. (2019). Organoid models for translational pancreatic cancer research. *Current Opinion in Genetics & Development, 54*, 7–11.

Vaseva, A. V., Blake, D. R., Gilbert, T. S. K., Ng, S., Hostetter, G., Azam, S. H., ... Der, C. J. (2018). KRAS suppression-induced degradation of MYC is antagonized by a MEK5-ERK5 compensatory mechanism. *Cancer Cell, 34*(5), 807–822.e7.

Wang, L., Zhao, L., Wei, G., Saur, D., Seidler, B., Wang, J., ... Qi, T. (2018). Homoharringtonine could induce quick protein synthesis of PSMD11 through activating MEK1/ERK1/2 signaling pathway in pancreatic cancer cells. *Journal of Cellular Biochemistry, 119*(8), 6644–6656.

Wang, X., Li, H., Lu, X., Wen, C., Huo, Z., Shi, M., ... Shen, B. (2018). Melittin-induced long non-coding RNA NONHSAT105177 inhibits proliferation and migration of pancreatic ductal adenocarcinoma. *Cell Death & Disease, 9*(10), 940.

Wang, Y. Z., Xu, W. W., Zhu, D. Y., Zhang, N., Wang, Y. L., Ding, M., ... Wang, X. X. (2018). Specific expression network analysis of diabetic nephropathy kidney tissue revealed key methylated sites. *Journal of Cellular Physiology, 233*(10), 7139–7147.

Xie, G., Wu, H., Cai, W., Chen, M., Huang, W., Yan, W., & Chang, Y. (2019). RDM1 promotes neuroblastoma growth through the RAS-Raf-MEK-ERK pathway. *FEBS Open Bio, 9*(3), 490–497.

Xing, W., Qi, Z., Huang, C., Zhang, N., Zhang, W., Li, Y., ... Hui, G. (2019). Genome-wide identification of lncRNAs and mRNAs differentially

expressed in non-functioning pituitary adenoma and construction of an lncRNA-mRNA co-expression network. *Biology Open*, *8*(1), bio037127.

Xiu, D. H., Liu, G. F., Yu, S. N., Li, L. Y., Zhao, G. Q., Liu, L., & Li, X. F. (2019). Long non-coding RNA LINC00968 attenuates drug resistance of breast cancer cells through inhibiting the Wnt2/β-catenin signaling pathway by regulating WNT2. *Journal of Experimental & Clinical Cancer Research*, *38*(1), 94.

Yin, L., Cai, Z., Zhu, B., & Xu, C. (2018). Identification of key pathways and genes in the dynamic progression of HCC based on WGCNA. *Genes*, *9*(2), E92.

Yu, X., Wang, D., Wang, X., Sun, S., Zhang, Y., Wang, S., … Qu, X. (2019). CXCL12/CXCR4 promotes inflammation-driven colorectal cancer progression through activation of RhoA signaling by sponging miR-133a-3p. *Journal of Experimental & Clinical Cancer Research*, *38*(1), 32.